Molecular Biology of the Cell
Vol. 19, 971–983, March 2008

The Interaction of JRAB/MICAL-L2 with Rab8 and Rab13 Coordinates the Assembly of Tight Junctions and Adherens Junctions

Rie Yamamura,*† Noriyuki Nishimura,* Hiroyoshi Nakatsuji,* Seiji Arase,† and Takuya Sasaki*

*Departments of Biochemistry and †Dermatology, Institute of Health Biosciences, The University of Tokushima Graduate School, Tokushima 770-8503, Japan

Submitted June 11, 2007; Revised November 5, 2007; Accepted December 6, 2007
Monitoring Editor: Asma Nusrat

The assembly of tight junctions (TJs) and adherens junctions (AJs) is regulated by the transport of integral TJ and AJ proteins to and/or from the plasma membrane (PM) and it is tightly coordinated in epithelial cells. We previously reported that Rab13 and a junctional Rab13-binding protein (JRAB)/molecule interacting with CasL-like 2 (MICAL-L2) mediated the endocytic recycling of an integral TJ protein occludin and the formation of functional TJs. Here, we investigated the role of Rab13 and JRAB/MICAL-L2 in the transport of other integral TJ and AJ proteins claudin-1 and E-cadherin to the PM by using a Ca^{2+}-switch model. Although knockdown of Rab13 specifically suppressed claudin-1 and occludin but not E-cadherin transport, knockdown of JRAB/MICAL-L2 and expression of its Rab13-binding domain (JRAB/MICAL-L2-C) inhibited claudin-1, occludin, and E-cadherin transport. We then identified Rab8 as another JRAB/MICAL-L2-C-binding protein. Knockdown of Rab8 inhibited the Rab13-independent transport of E-cadherin to the PM. Rab8 and Rab13 competed with each other for the binding to JRAB/MICAL-L2 and functionally associated with JRAB/MICAL-L2 at the perinuclear recycling/storage compartments and PM, respectively. These results suggest that the interaction of JRAB/MICAL-L2 with Rab8 and Rab13 coordinates the assembly of AJs and TJs.

INTRODUCTION

Tight junctions (TJs) and adherens junctions (AJs) are located at the apical end of the basolateral membrane of polarized epithelial cells. Epithelial polarization entails a complex interplay between the coordinated assembly of TJs and AJs, and several fundamental cellular processes. These include the activation of evolutionarily conserved polarity protein complexes, the reorganization of actin and microtubule cytoskeletons, the redistribution of organelles, and the polarization of membrane traffic. During a series of processes, epithelial cells first form spot-like primordial AJs at the tips of the initial cell–cell contacts, and they develop belt-like mature AJs. In parallel with the maturation of AJs, TJs are formed at the apical side of AJs (Yap *et al*., 1997; Vasioukhin *et al*., 2000; Nelson, 2003; Takai and Nakanishi, 2003). However, the molecular mechanism that coordinates the assembly of TJs and AJs remains to be clarified.

While AJs principally initiate and maintain cell–cell contacts, TJs seal the intercellular space and delineate the boundaries between the apical and basolateral membranes. Both TJs and AJs are composed of integral membrane proteins and plaque proteins associated with the cytosolic side of the plasma membrane. The principal integral TJ and AJ proteins are claudins and E-cadherin, which form homophilic interactions with the same family of proteins on an adjacent cell to form the characteristic structures of TJs and AJs, respectively (Takeichi, 1995; Yap *et al*., 1997; Tsukita *et al*., 2001). Additional integral TJ and AJ proteins include occludin, junctional adhesion molecules, and nectins (Takai and Nakanishi, 2003; Ebnet *et al*., 2004). These integral membrane proteins are linked to a number of TJ and AJ plaque proteins in the cytosol, including zonula occludens (ZO) proteins (ZO-1, ZO-2, and ZO-3) and catenins, which in turn bind the actin cytoskeleton. These TJ and AJ plaque proteins have multiple protein binding motifs, and they form an organizing platform for a variety of scaffolding, signaling, and membrane trafficking proteins (Gonzalez-Mariscal *et al*., 2003).

Accumulating evidence has revealed that the membrane trafficking of integral TJ and AJ proteins plays a key role in the assembly and maintenance of TJs and AJs (Ivanov *et al*., 2005). Among a number of membrane trafficking proteins identified, Rab family small G proteins are key regulators (Takai *et al*., 2001; Zerial and McBride, 2001; Pfeffer and Aivazian, 2004). More than 60 different Rab family members have been identified in mammalian cells, and each member recognizes distinct subsets of intracellular membranes. Rab proteins cycle between the "inactive" guanosine diphosphate (GDP)-bound and "active" guanosine triphosphate (GTP)-bound forms, and they also undergo a membrane insertion and extraction cycle, allowing both spatial and temporal control of their activity. GTP-bound Rab proteins interact with specific effector proteins, and together they act

This article was published online ahead of print in *MBC in Press* (http://www.molbiolcell.org/cgi/doi/10.1091/mbc.E07–06–0551) on December 19, 2007.

Address correspondence to: Takuya Sasaki (sasaki@basic.med.tokushima-u.ac.jp).

Abbreviations used: AJ, adherens junction; CC, coiled-coil; PM, plasma membrane; siRNA, small interfering RNA; TfR, transferrin receptor; TJ, tight junction; ZO, zonula occludens.

to translate the signal from one Rab protein to several diverse components of membrane trafficking. In epithelial cells, Rab8 and Rab13 are identified as AJ and TJ plaque proteins (Zahraoui *et al*., 1994; Lau and Mruk, 2003). While Rab8 localizes to the *trans*-Golgi network, recycling endosomes, vesicular and tubular structures in the cytosol, membrane protrusions, and plasma membrane (PM) in addition to AJs (Huber *et al*., 1993b; Lau and Mruk, 2003; Ang *et al*., 2004), Rab13 resides at perinuclear membrane structures, vesicular structures in the cytosol, and PM in addition to TJs (Zahraoui *et al*., 1994; Marzesco *et al*., 2002; Terai *et al*., 2006). Rab8 interacts with Rab8ip/germinal center kinase (GCK), JFC1/Slp1, and Optineurin in a GTP-dependent manner (Ren *et al*., 1996; Hattula and Peränen, 2000; Hattula *et al*., 2006), and it is implicated in multiple transport pathways, including the epithelial-specific adaptor protein complex AP-1B-dependent basolateral transport, the polarized membrane traffic to the dendritic membrane, the actin-dependent movement of melanosomes, the formation and destruction of membrane protrusions, and the cell–cell adhesion (Huber *et al*., 1993a; Ang *et al*., 2003; Powell and Temesvari, 2004; Chabrillat *et al*., 2005; Hattula *et al*., 2006). Rab13 also binds to protein kinase A (PKA), and it regulates the assembly of functional TJs, neurite outgrowth, and neuronal regeneration (Marzesco *et al*., 2002; Köhler *et al*., 2004; Di Giovanni *et al*., 2005). However, the exact transport routes regulated by Rab8 and Rab13 remain to be determined.

Claudins, occludin, and E-cadherin are transported to and from the PM by multiple exocytic and endocytic pathways. For their transport from the PM, three distinct endocytosis pathways—clathrin-dependent endocytosis, caveolin-dependent endocytosis, and macropinocytosis—are identified in different cellular contexts (Bryant and Stow, 2004; D'Souza-Schorey, 2005; Ivanov *et al*., 2005). Endocytosed claudins, occludin, and E-cadherin are also detected in multiple sites, including early endosome antigen (EEA)1-positive early endosomes, Rab11-positive recycling endosomes, Rab7-positive late endosomes, Rab13-positive vesicles, Syntaxin4-positive compartments, and Syntaxin3-positive vacuolar apical compartments (Le *et al*., 1999; Harhaj *et al*., 2002; Hopkins *et al*., 2003; Ivanov *et al*., 2004; Matsuda *et al*., 2004; Balzac *et al*., 2005; Bruewer *et al*., 2005; Morimoto *et al*., 2005; Utech *et al*., 2005). From these sites, claudins, occludin, and E-cadherin can be transported to the PM. Although a variety of regulatory molecules, including actin and microtubule cytoskeletons, myosin II, Rac1, Cdc42, ARF6, and Rab11 have been identified, the exact transport routes of claudins, occludin, and E-cadherin to and from the PM are not defined (Bryant and Stow, 2004; D'Souza-Schorey, 2005; Ivanov *et al*., 2005).

We previously reported that Rab13 regulated the endocytic recycling of occludin, and we identified a junctional Rab13-binding protein (JRAB)/molecule interacting with CasL-like 2 (MICAL-L2) as a novel Rab13 effector protein (Morimoto *et al*., 2005; Terai *et al*., 2006). Although JRAB/MICAL-L2 was originally identified as a MICAL-related cDNA (Terman *et al*., 2002), it also mediated the endocytic recycling of occludin and regulated the formation of functional TJs in epithelial cells (Terai *et al*., 2006). In the present study, we investigated the role of Rab13 and JRAB/MICAL-L2 in the transport of claudins and E-cadherin to the PM by using a well-established Ca^{2+}-switch model (Kartenbeck *et al*., 1991). Although Rab13 specifically mediated claudin but not E-cadherin transport, JRAB/MICAL-L2 regulated both claudin and E-cadherin transport. We then identified Rab8 as an additional JRAB/MICAL-L2 effector protein that controlled the Rab13-independent transport of E-cadherin.

MATERIALS AND METHODS

Plasmid Construction

The mammalian expression vectors pCI-neo-Myc-JRAB/MICAL-L2-F, pCI-neo-Myc-JRAB/MICAL-L2-C, pCI-neo-HA-Rab1A, pCI-neo-HA-Rab3B, pCI-neo-HA-Rab5A, and pCI-neo-HA-Rab13 were described previously (Yamamoto *et al*., 2003; Terai *et al*., 2006). Rab13 cDNA was cloned into the pGEX-6P-1, pCI-neo-Myc, and pCI-neo-FLAG vectors. JRAB/MICAL-L2-CC (amino acids 806-912) and JRAB/MICAL-L2-CT (amino acids 913-1009) cDNAs were generated by polymerase chain reaction (PCR) by using pCI-neo-Myc-JRAB/MICAL-L2-F as a template, and they were then cloned into the pCI-neo-Myc vector. Mouse Rab8A cDNA was amplified by PCR by using a yeast two-hybrid prey clone (pACT2-Rab8A) as a template, and then it was cloned into pCI-neo-HA, pCI-neo-Myc, and pCI-neo-FLAG vectors. Canine Rab4A, mouse Rab8B, mouse Rab10, and rat Rab11A cDNAs were isolated by reverse transcription (RT)-PCR from Madin-Darby canine kidney (MDCK) cells, NIH3T3 cells, MTD-1A cells, and rat brain, respectively, and then they were cloned into the pCI-neo-HA vector. cDNAs for mouse MICAL-1 (Q8VDP3, 1048 amino acids), mouse MICAL-3 (Q8CJ19, 864 amino acids), and mouse MICAL-L1 (Q8BGT6, 870 amino acids) were isolated by RT-PCR from mouse lung, mouse brain, and MTD-1A cells, respectively. Mouse MICAL-2 (Q8BML1, 960 amino acids) cDNA was generated by PCR by using the RIKEN FANTOM clone 5330438E18 (DNAFORM, Ibaraki, Japan) as a template. MICAL-1, MICAL-2, MICAL-3, and MICAL-L1 cDNAs were cloned into the pCI-neo-Myc and pCI-neo-HA vectors. All plasmids constructed in this study were sequenced using an ABI Prism 3100 Genetic Analyzer (Applied Biosystems, Foster City, CA).

Antibodies

Glutathione-S-transferase (GST) and N-terminal GST-tagged Rab13 (GST-Rab13) proteins were expressed from the pGEX-6P-1 (GE Healthcare, Piscataway, NJ) vector in *Escherichia coli* strain DH5α and purified by using glutathione-Sepharose beads (GE Healthcare) according to the manufacturer's instructions. Two milligrams of GST or GST–Rab13 protein were immobilized on HiTrap NHS-activated columns (GE Healthcare) according to the manufacturer's instructions. Two female Wistar rats were immunized with 100 μg of GST–Rab13 protein twice at 4-wk intervals, after which whole blood from the animals was collected. Crude immunoglobulin fractions were prepared by ammonium sulfate precipitation and passed through a GST-immobilized column to remove any anti-GST antibody. The anti-Rab13 polyclonal antibody was further purified on a GST–Rab13-immobilized column according to the manufacturer's instructions. The rat anti-JRAB/MICAL-L2 antibody was described previously (Terai *et al*., 2006). The rat anti-occludin (MOC37) antibody was the kind gift from Dr. S. Tsukita (Kyoto University, Kyoto, Japan). Rabbit anti-claudin-1 and rabbit anti-ZO-1 were purchased from Zymed Laboratories (San Francisco, CA); rat anti-E-cadherin was from Takara (Otsu, Japan); mouse anti-EEA1 and mouse anti-Rab8 were from BD Biosciences (San Jose, CA); mouse anti-Golgi 58K, mouse anti-β-actin, and mouse anti-FLAG (M2) were from Sigma-Aldrich (St. Louis, MO); mouse anti-mannose 6-phosphate receptor (M6PR) was from Affinity BioReagents (Golden, CO); mouse anti-Myc (9E10) was from American Type Culture Collection (Manassas, VA); mouse anti-hemagglutinin (HA) (12CA5) and rat anti-HA (3F10) were from Roche Diagnostics (Mannheim, Germany); and rabbit anti-green fluorescent protein (GFP) was from Invitrogen (Carlsbad, CA).

Cell Culture and Transfection

MDCK, MDCK I, and MTD-1A cells were kindly supplied by Dr. W. Birchmeier (Max Delbrueck Center for Molecular Medicine, Berlin, Germany), Dr. T. Tsukamoto (Kitano Hospital, Osaka, Japan), and Dr. S. Tsukita (Kyoto University, Kyoto, Japan), respectively. Baby hamster kidney (BHK) and NIH3T3 cells were obtained from American Type Culture Collection. MDCK, MTD-1A, and BHK cells were cultured in DMEM with 10% fetal bovine serum (FBS), and MDCK I cells were cultured in DMEM with 5% FBS. MDCK, MDCK I, MTD-1A, and BHK cells were transfected using a Nucleofector device (Amaxa, Köln, Germany) or with Lipofectamine 2000 transfection reagent (Invitrogen) according to the manufacturers' instructions.

Recombinant Adenovirus Infection

The recombinant adenovirus expressing enhanced green fluorescent protein (EGFP) and Myc-JRAB/MICAL-L2-C (Ad-EGFP and Ad-Myc-JRAB/MICAL-L2-C) was described previously (Terai *et al*., 2006). MTD-1A cells were infected with Ad-EGFP or Ad-Myc-JRAB/MICAL-L2-C at a multiplicity of infection of 100.

RNA Interference

The 21-mer small interfering RNA (siRNA) duplexes targeting canine Rab13 (XM_850035), mouse JRAB/MICAL-L2 (AB182579), canine Rab8A (NM_001003152), canine MICAL-1 (XM_539079), canine MICAL-L1 (XM_538381), and canine JRAB/MICAL-L2 (XM_547017) and the control nonsilencing siRNA duplexes were obtained from B-Bridge (Sunnyvale, CA), and they were transfected using a Nucleofector device (Amaxa) according to the manufacturer's instructions. The target

sequences were as follows: canine Rab13 (#1, 5′-GAGGACAGCTTCAACAACA-3′; #2, 5′-GACAATAACTACTGCATAT-3′; and #3, 5′-GCGCCTGCTTCTAGGGAAC-3′), mouse JRAB/MICAL-L2 (#1, 5′-GGACAAACCCTGTGGTTCA-3′; #2, 5′-GGACGGTTCAGGAGGCAAA-3′; and #3, 5′-GGCTGAAGCCTGTGGATAA-3′), canine Rab8A (#1, 5′-CCATAGAGCTCGATGGCAA-3′; #2, 5′-GCAAGAGAATTA-AGCTACA-3′; and #3, 5′-GGAATCAAGTTCATGGAGA-3′), canine MICAL-1 (5′-GTGGTGAACCAGCGAGATA-3′), canine MICAL-L1 (5′-GAGAGAAGGTGCT-GATGCA-3′), and canine JRAB/MICAL-L2 (5′-GCAGCAACATCGTGGACGT-3′).

Quantitative Real-Time RT-PCR

Total RNA from MDCK cells transfected with control RNA, MICAL-1 siRNA, MICAL-L1 siRNA, and JRAB/MICAL-L2 siRNA duplexes were isolated using BioRobot EZ1 with RNA Universal Tissue kit (QIAGEN, Valencia, CA) and reverse transcribed using QuantiTect Reverse Transcription kit (QIAGEN) according to the manufacturers' instructions. Real-time PCR analysis was performed with an ABI 7500 Real-Time PCR System (Applied Biosystems) by using FastStart Universal SYBR Green Master (Roche Diagnostics) according to the manufacturer's specifications. Each sample was analyzed in triplicates for each pair of primers. The relative expression of MICAL-1, MICAL-L1, and JRAB/MICAL-L2 to glyceraldehyde-3-phosphate dehydrogenase (GAPDH) was calculated by the relative standard curve method using Sequence Detection Software version 1.4 (Applied Biosystems). Primer sequences were as follows: canine MICAL-1 (forward, 5′-ACCAG-GAAGGAGCCCTAAAG-3′ and reverse, 5′-CTCCTGGAAGCGGATAAGTG-3′), canine MICAL-L1 (forward, 5′-CAAGATGTTGGAAGCCATGA-3′ and reverse, 5′-TAGCAGCTTCAGCACCTTCA-3′), canine JRAB/MICAL-L2 (forward, 5′-CACCTCGTGCAGAGACACCT-3′ and reverse: 5′-GTGCAGTGT-GTTGGAGCACT-3′), and canine GAPDH (forward, 5′-TCAACGGATTTG-GCCGTATTGG-3′ and reverse: 5′-TGAAGGGGTCATTGATGGCG-3′).

Ca^{2+}-Switch Assay

Ca^{2+}-switch assay was performed as described previously (Kartenbeck *et al*., 1991). Briefly, MTD-1A or MDCK cells were grown in DMEM with 10% FBS (normal Ca^{2+} ion medium [NCM]) and sequentially incubated in Ca^{2+}-free minimal essential medium without FBS (low Ca^{2+} ion medium [LCM]) for 1 h and in LCM with 20 mM EGTA (for MTD-1A cells) or 5 mM EGTA (for MDCK cells) for 2 h to remove extracellular Ca^{2+}. Cells were then incubated in NCM for varying periods and processed for immunofluorescence microscopy. Experiments in the presence of cycloheximide were performed by incubating MDCK cells sequentially with LCM, LCM containing 5 mM EGTA and 20 μM cycloheximide, and NCM containing 20 μM cycloheximide.

Transferrin Uptake

MDCK cells were cultured in serum-free DMEM for 1 h, incubated with 50 μg/ml Alexa 488-transferrin (Alexa-Tf; Invitrogen) for 1 h, and subjected to either a Ca^{2+}-switch assay in the continuous presence of 50 μg/ml Alexa-Tf or immunofluorescence microscopy.

Immunofluorescence Microscopy

MDCK and MTD-1A cells were grown on glass coverslips and fixed with one of the following: −20°C methanol (for anti-claudin-1 antibody) on ice for 5 min, 1% formaldehyde (for anti-occludin antibody) in phosphate-buffered saline (PBS) at room temperature for 15 min, or 2% formaldehyde (for other antibodies) in PBS at room temperature for 15 min. After permeabilization with 0.2% Triton X-100 in PBS for 15 min and blocking with 5% goat serum in PBS for 60 min, cells were incubated with primary antibodies for 60 min and with Alexa 488-, or Alexa 594-conjugated secondary antibodies (Invitrogen) at room temperature for 60 min. For triple-labeling, anti-FLAG (M2) antibody was labeled with Pacific Blue by using a Zenon antibody labeling kit (Invitrogen). Fluorescent images were acquired using a Radiance 2000 confocal laser-scanning microscope (Bio-Rad, Hercules, CA) or a C1plus confocal laser-scanning microscope (Nikon, Tokyo, Japan).

Quantitation of Claudin-1, Occludin, and E-Cadherin Length

To quantify the mean length of claudin-1, occludin, and E-cadherin per cell, the fields were randomly selected from fluorescent images to contain >100 cells. Total length of claudin-1, occludin, and E-cadherin at cell–cell contact sites was measured using Lumina Vision 2.4 program (Mitani, Fukui, Japan), and the mean length per cell was calculated by total length/total cell number. Statistical analysis was performed using Student's *t* test.

Ratio of Colocalized Area

To calculate the ratio of colocalized area, the fields were selected from fluorescent images to contain >100 cells. The JRAB/MICAL-L2-E-cadherin and JRAB/MICAL-L2-occludin colocalized area at perinuclear recycling/storage compartment (PNC) and PM was measured using Lumina Vision 2.4 program (Mitani). Although the colocalized structures that positioned at cell–cell contact sites were defined as PM, all other colocalized structures were defined as PNC. Ratio was calculated by colocalized area at PNC/colocalized area at PM.

Measurement of Transepithelial Electrical Resistance (TER)

MDCK I cells (8×10^4) transfected with control RNA, MICAL-1 siRNA, MICAL-L1 siRNA, or JRAB/MICAL-L2 siRNA were plated onto Transwell filters (polycarbonate membranes with 12-mm diameter and 0.4-μm pore size; Corning Life Sciences, Acton, MA) and grown in NCM for 72–96 h and subjected to a Ca^{2+}-switch assay in which the incubation in LCM with 5 mM EGTA was shortened to 10 min. TER was measured directly in culture media at 6 and 12 h after restoring Ca^{2+} by using a Millicell-ERS epithelial voltohmmeter (Millipore, Billerica, MA). TER values were calculated by subtracting the background TER of blank filters and by multiplying the surface area of the filter.

Two-Hybrid Screening

JRAB/MICAL-L2-C was cloned into the yeast two-hybrid bait vector pGBDU-C1 (James *et al*., 1996). A mouse 11-d-old embryo cDNA library in the yeast two-hybrid prey vector pACT2 was purchased from Clontech (Palo Alto, CA). The yeast strain PJ69-4A (*MATa trp1-901 leu2-3112 ura3-52 his3-200 gal4Δ gal80Δ GAL2-ADE2 LYS2::GAL1-HIS3 met2::GAL7-lacZ*) was sequentially transformed with pGBDU-JRAB/MICAL-L2-C and the mouse 11-d-old embryo cDNA library. Two-hybrid screening was performed and evaluated as described previously (James *et al*., 1996).

Coimmunoprecipitation

BHK and MTD-1A cells were lysed with 25 mM Tris/HCl, pH 7.5, containing 0.5% 3-[(3-cholamidopropyl)dimethylammonio]propanesulfonate (CHAPS), 125 mM NaCl, 1 mM $MgCl_2$, 20 μg/ml (4-amidinophenyl)-methanesulfonyl fluoride, and 100 μM guanosine 5′-*O*-(3-thio)triphosphate (GTPγS)/GDP at 4°C for 15 min. After removing a fraction of the lysates, the remaining lysates were immunoprecipitated with the indicated antibodies bound to protein G-Sepharose beads (GE Healthcare) and washed three times with 25 mM Tris/HCl, pH 7.5, containing 0.1% CHAPS, 300 mM NaCl, 1 mM $MgCl_2$, and 10 μM GTPγS/GDP. The samples were prepared for Western blot analysis.

Western Blot

Proteins were separated by SDS-polyacrylamide gel electrophoresis, and proteins were transferred to polyvinylidene difluoride membranes. Membrane blocking and antibody dilutions were done in Block Ace (Dainippon Pharmaceutical, Osaka, Japan). Blots were developed by chemiluminescence using a horseradish peroxidase-coupled secondary antibody (Jackson ImmunoResearch Laboratories, West Grove, PA) and Immobilon Western Chemiluminescent Horseradish Peroxidase Substrate (Millipore).

RESULTS

Rab13 Is Involved in the Transport of Claudin-1 and Occludin, but not E-Cadherin, to the PM

We previously reported that Rab13 and JRAB/MICAL-L2 specifically regulated the endocytic recycling of occludin and the assembly of functional TJs (Terai *et al*., 2006). Because claudins but not occludin are recognized as the primary integral TJ proteins and the simultaneous and/or orchestrated endocytosis of integral TJ and AJ proteins is observed in a variety of physiological and pathological conditions (Ivanov *et al*., 2005), the question has naturally arisen as to whether Rab13 and JRAB/MICAL-L2 also regulate the transport of claudins and E-cadherin to the PM. In the present study, we have used a well established Ca^{2+}-switch model (Kartenbeck *et al*., 1991) to investigate the transport of claudins, occludin, and E-cadherin to the PM. MDCK or MTD-1A cells were first incubated in Ca^{2+}-chelated medium to internalize claudins, occludin, and E-cadherin from the PM and to induce the disassembly of cell–cell junctions. Subsequently, they were cultured in physiological Ca^{2+} medium to transport claudins, occludin, and E-cadherin to the PM and to induce the synchronous assembly of cell–cell junctions. The localizations of claudin-1, occludin, and E-cadherin were then analyzed by immunofluorescence microscopy at 0, 2, 4, 6, and 24 h after the restoration of physiological Ca^{2+}.

To examine the role of Rab13, we designed siRNAs against the canine Rab13 sequence (XM_850035), and we transfected them into MDCK cells. All Rab13 siRNAs sup-

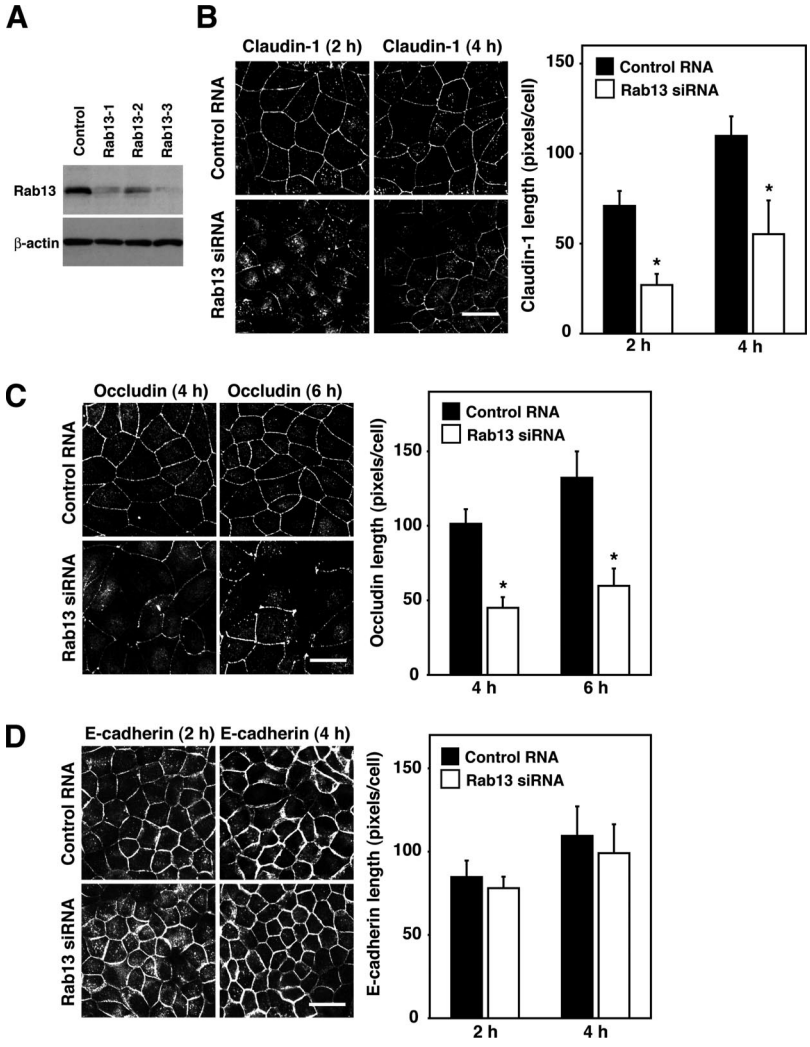

Figure 1. Rab13 is involved in the transport of claudin-1 and occludin, but not E-cadherin, to the PM. (A) MDCK cells were transfected with control RNA or Rab13 siRNA and subjected to Western blot analysis by using anti-Rab13 and anti-β-actin antibodies. The result shown is representative of three independent experiments. (B–D) MDCK cells transfected with control RNA or Rab13 siRNA were subjected to a Ca^{2+}-switch assay and then immunostained with anti-claudin-1, anti-occludin, and anti-E-cadherin antibodies at the indicated time after Ca^{2+} restoration. Representative images of three independent experiments are shown. Bars, 20 μm. Claudin-1, occludin, and E-cadherin length is quantified and shown as the mean and SEM. The asterisks denote a significant difference between control RNA and Rab13 siRNA ($p < 0.05$).

pressed the expression of Rab13 protein in MDCK cells, whereas a nonsilencing control RNA did not (Figure 1A). The most effective Rab13-3 siRNA was used in the present study. In MDCK cells transfected with control RNA or Rab13 siRNA, claudin-1, occludin, and E-cadherin internalized from the PM and accumulated intracellularly after Ca^{2+} removal, and each was then transported to the PM within 24 h of Ca^{2+} restoration (Supplemental Figure S1, A–C). However, the kinetics of the transport of claudin-1 and occludin to the PM seemed different. In accordance with previous reports using a GTP hydrolysis-defective mutant of Rab13 (Rab13 Q67L) (Marzesco *et al*., 2002; Terai *et al*., 2006), the depletion of Rab13 slowed the kinetics of claudin-1 and occludin transport to the PM at 2, 4, and 6 h after Ca^{2+} restoration (Figure 1, B and C). In marked contrast, the disappearance of the intracellular staining of and/or the appearance of continuous PM staining of E-cadherin was indistinguishable between Rab13-depleted and control cells at 2 and 4 h after Ca^{2+} restoration (Figure 1D). These results demonstrated that Rab13 was specifically required for the transport of claudin-1 and occludin, but not E-cadherin, to the PM.

JRAB/MICAL-L2 Is Involved in the Transport of Claudin-1, Occludin, and E-Cadherin to the PM

We next addressed the role of JRAB/MICAL-L2 in the transport of claudin-1, occludin, and E-cadherin to the PM by using a Ca^{2+}-switch assay. To this end, we designed three siRNAs targeting the mouse JRAB/MICAL-L2 sequence (AB182579). Transfection of all three JRAB/MICAL-L2 siRNAs reduced the expression of JRAB/MICAL-L2 relative to a nonsilencing control RNA in MTD-1A cells (Figure 2A). The JRAB/MICAL-L2-3 siRNA suppressed the expression of JRAB/MICAL-L2 most efficiently, so it was used in the present study. Next, we investigated the transport of claudin-1, occludin, and E-cadherin to the PM during the Ca^{2+} switch in control and JRAB/MICAL-L2-depleted MTD-1A cells. In contrast to Rab13-depleted cells, the knockdown of JRAB/MICAL-L2 considerably delayed the disappearance of intracellular staining and/or the appearance of continuous PM staining of claudin-1, occludin, and E-cadherin (Figure 2, B–D, and Supplemental Figure S2, A–C), indicating that JRAB/MICAL-L2 is required for the transport of claudin-1, occludin, and E-cadherin to the PM.

Expression of the Rab13-binding Domain of JRAB/MICAL-L2 Inhibits the Transport of Claudin-1, Occludin, and E-Cadherin to the PM

The above-mentioned results clearly demonstrated that both Rab13 and JRAB/MICAL-L2 controlled the transport of claudin-1 and occludin to the PM. However, it also revealed that JRAB/MICAL-L2 possessed the Rab13-independent

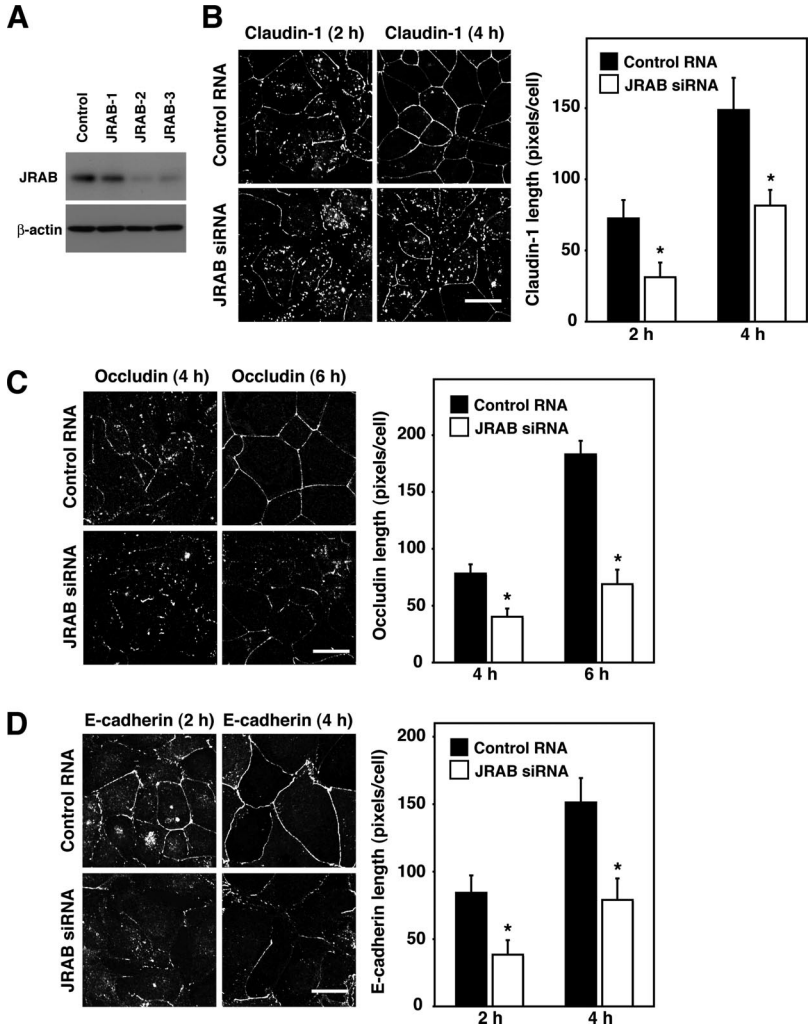

Figure 2. JRAB/MICAL-L2 is involved in the transport of claudin-1, occludin, and E-cadherin to the PM. (A) MTD-1A cells were transfected with control RNA or JRAB/MICAL-L2 siRNA and subjected to Western blot analysis by using anti-JRAB/MICAL-L2 and anti-β-actin antibodies. The result shown is representative of three independent experiments. (B–D) MTD-1A cells transfected with control RNA or JRAB/MICAL-L2 siRNA were subjected to a Ca^{2+}-switch assay and then immunostained with anti-claudin-1, anti-occludin, and anti-E-cadherin antibodies at the indicated time after Ca^{2+} restoration. Representative images of three independent experiments are shown. Bars, 20 μm. Claudin-1, occludin, and E-cadherin length is quantified and shown as the mean and SEM. The asterisks denote a significant difference between control RNA and JRAB/MICAL-L2 siRNA ($p < 0.05$).

function related to the transport of E-cadherin to the PM. To explore its molecular mechanism, we first expressed the Rab13-binding domain of JRAB/MICAL-L2 (JRAB/MICAL-L2-C) in MTD-1A cells and examined its effect on the transport of claudin-1, occludin, and E-cadherin to the PM by using a Ca^{2+}-switch assay (Figure 3A). Compared with GFP-expressing MTD-1A cells, the appearance of continuous PM staining of claudin-1, occludin, and E-cadherin was substantially delayed in JRAB/MICAL-L2-C–expressing cells (Figure 3, B–D, and Supplemental Figure S3, B–D). Importantly, JRAB/MICAL-L2-C efficiently blocked the Rab13-independent transport of E-cadherin to the PM.

Rab8 Is Identified as Another JRAB/MICAL-L2-binding Protein that Mediates the Rab13-independent Transport of E-Cadherin to the PM

Because JRAB/MICAL-L2-C inhibited the Rab13-independent function of JRAB/MICAL-L2, it might interact with other molecules in addition to Rab13. To test this possibility, we screened a yeast two-hybrid library constructed from a mouse 11-d-old embryo cDNA by using JRAB/MICAL-L2-C as bait. From the 4.1×10^6 clones screened, we obtained two independent clones encoding the mouse Rab8A sequence in addition to nine independent clones encoding the mouse Rab13 sequence. Both Rab8A prey clones encoded the full-length mouse Rab8A sequence and specifically bound JRAB/MICAL-L2-C (Figure 4A).

To confirm the yeast two-hybrid interaction between Rab8A and JRAB/MICAL-L2 in intact cells, we next performed coimmunoprecipitation experiments. When HA-tagged Rab8A (HA-Rab8A) was cotransfected with Myc-tagged JRAB/MICAL-L2 (Myc-JRAB/MICAL-L2-F) into BHK cells, Myc-JRAB/MICAL-L2-F was specifically coimmunoprecipitated with HA-Rab8A in the presence of GTPγS, but not GDP (Figure 4B). Endogenous Rab8 was also immunoprecipitated from MTD-1A cells with the anti-JRAB/MICAL-L2 antibody (Supplemental Figure S4A). Because single Rab effector protein can interact with closely related multiple Rab proteins (Fukuda, 2003), we then examined the interaction of JRAB/MICAL-L2 with other Rab proteins. When Myc-JRAB/MICAL-L2 was coexpressed with HA-Rab1A, HA-Rab3B, HA-Rab5A, HA-Rab8A, HA-Rab8B, HA-Rab10, or HA-Rab13 in BHK cells, it coimmunoprecipitated with HA-Rab8A, HA-Rab8B, and HA-Rab13, but not with HA-Rab1A, HA-Rab3B, HA-Rab5A, and HA-Rab10 (Figure 4C). We further investigated the interaction of JRAB/MICAL-L2 with Rab proteins implicated in the regulation of endocytic recycling. When HA-Rab4A, HA-Rab8A, HA-Rab11A, and HA-Rab13 were expressed in MTD-1A cells, endogenous JRAB/MICAL-L2 specifically interacted

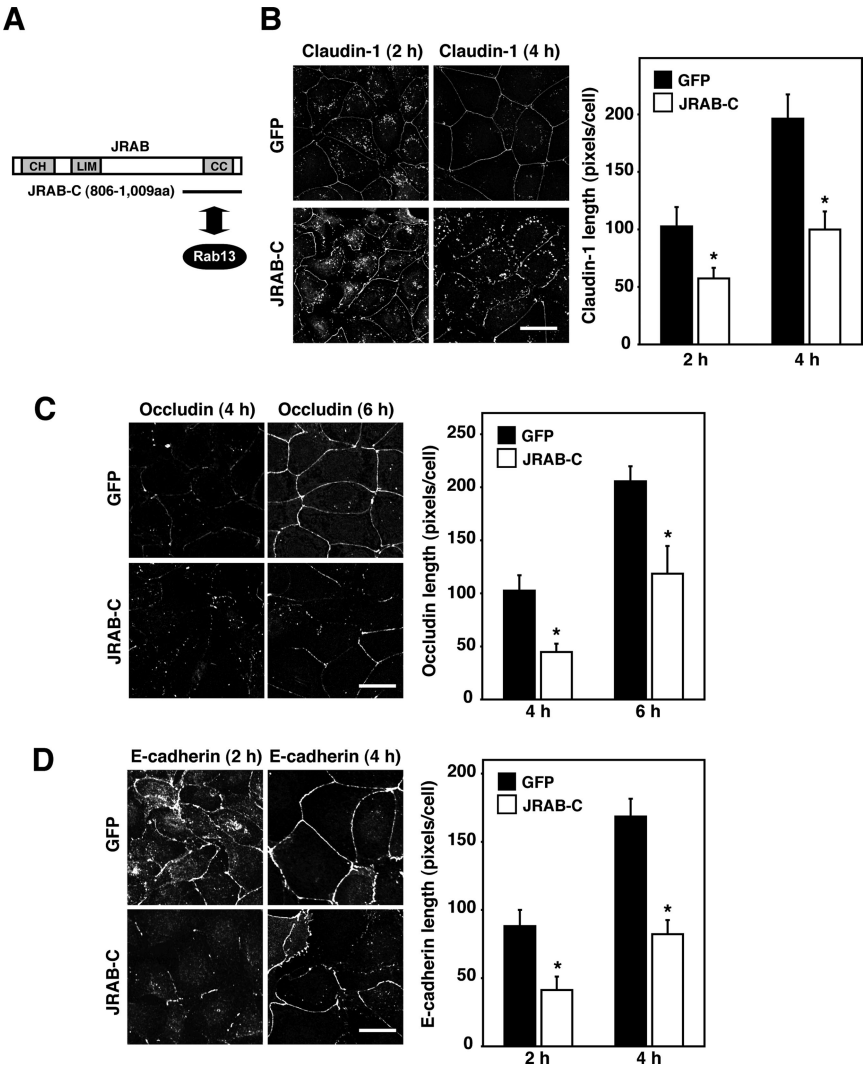

Figure 3. Expression of the Rab13-binding domain of JRAB/MICAL-L2 inhibits the transport of claudin-1, occludin, and E-cadherin to the PM. (A) The Rab13-binding domain of JRAB/MICAL-L2. CH, calponin homology domain; LIM, LIM domain; and CC, coiled-coil domain. (B–D) MTD-1A cells infected with Ad-EGFP (GFP) or Ad-Myc-JRAB/MICAL-L2-C (JRAB-C) were subjected to a Ca^{2+}-switch assay, and then they were immunostained with anti-claudin-1, anti-occludin, and anti-E-cadherin antibodies at the indicated time after Ca^{2+} restoration. Representative images of three independent experiments are shown. Bars, 20 μm. Claudin-1, occludin, and E-cadherin length is quantified and shown as the mean and SEM. The asterisks denote a significant difference between GFP and JRAB/MICAL-L2-C ($p < 0.05$).

with HA-Rab8A and HA-Rab13, but not with HA-Rab4A and HA-Rab11A (Figure 4D). These results suggested that JRAB/MICAL-L2 specifically interacted with Rab8 and Rab13 in epithelial cells.

If JRAB/MICAL-L2 mediated the Rab13-independent transport of E-cadherin to the PM and also interacted with Rab8A, Rab8A was possibly involved. To test this possibility, we designed three siRNAs targeting the canine Rab8A sequence (NM_001003152). Although all Rab8A siRNAs suppressed the expression of Rab8A protein in MDCK cells relative to a nonsilencing control RNA, the Rab8A-3 siRNA was the most effective and used in the present study (Supplemental Figure S4B). When we examined the transport of E-cadherin to the PM during the Ca^{2+} switch in control and Rab8A-depleted MDCK cells, it was substantially delayed in Rab8A-depleted cells relative to control cells (Figure 4E and Supplemental Figure S4C).

MICAL Family Proteins Specifically Interacts with Rab Family Proteins

Because JRAB/MICAL-L2 is a member of MICAL family proteins that is conserved from flies to mammals, with two MICAL family genes (D-MICAL and D-MICAL-L) identified in *Drosophila* and five (MICAL-1, MICAL-2, MICAL-3, MICAL-L1, and JRAB/MICAL-L2) found in mammals (Figure 5A) (Suzuki *et al*., 2002; Terman *et al*., 2002), we further investigated the interaction of Rab8A and Rab13 with other MICAL family proteins. HA-Rab8A or HA-Rab13 was coexpressed with Myc-MICAL-1, Myc-MICAL-2, Myc-MICAL-3, Myc-MICAL-L1, or Myc-JRAB/MICAL-L2 in BHK cells and analyzed by coimmunoprecipitation. Although HA-Rab8A precipitated with Myc-MICAL-1, Myc-MICAL-L1, and Myc-JRAB/MICAL-L2 but not with Myc-MICAL-2 and Myc-MICAL-3, HA-Rab13 preferentially interacted with Myc-JRAB/MICAL-L2 (Figure 5, B and C). To explore the physiological significance of these interactions, we next examined the role of MICAL-1, MICAL-L1, and JRAB/MICAL-L2 on the development of TER, which is often used to monitor the tightness of the seal created by functional TJs. For this purpose, we designed siRNAs targeting canine MICAL-1 (XM_539079), MICAL-L1 (XM_538381), and JRAB/MICAL-L2 (XM_547017), and we monitored their effect by quantitative real-time RT-PCR. MICAL-1, MICAL-L1, and JRAB/MICAL-L2 siRNAs efficiently suppressed the mRNA expression compared with a nonsilencing control RNA, and were used in the present study (Figure 5D). When cultured on permeable filters for 72–96 h, all MDCK I cells transfected with control RNA, MICAL-1 siRNA, MICAL-L1 siRNA, and JRAB/MICAL-L2 siRNA showed the high TER

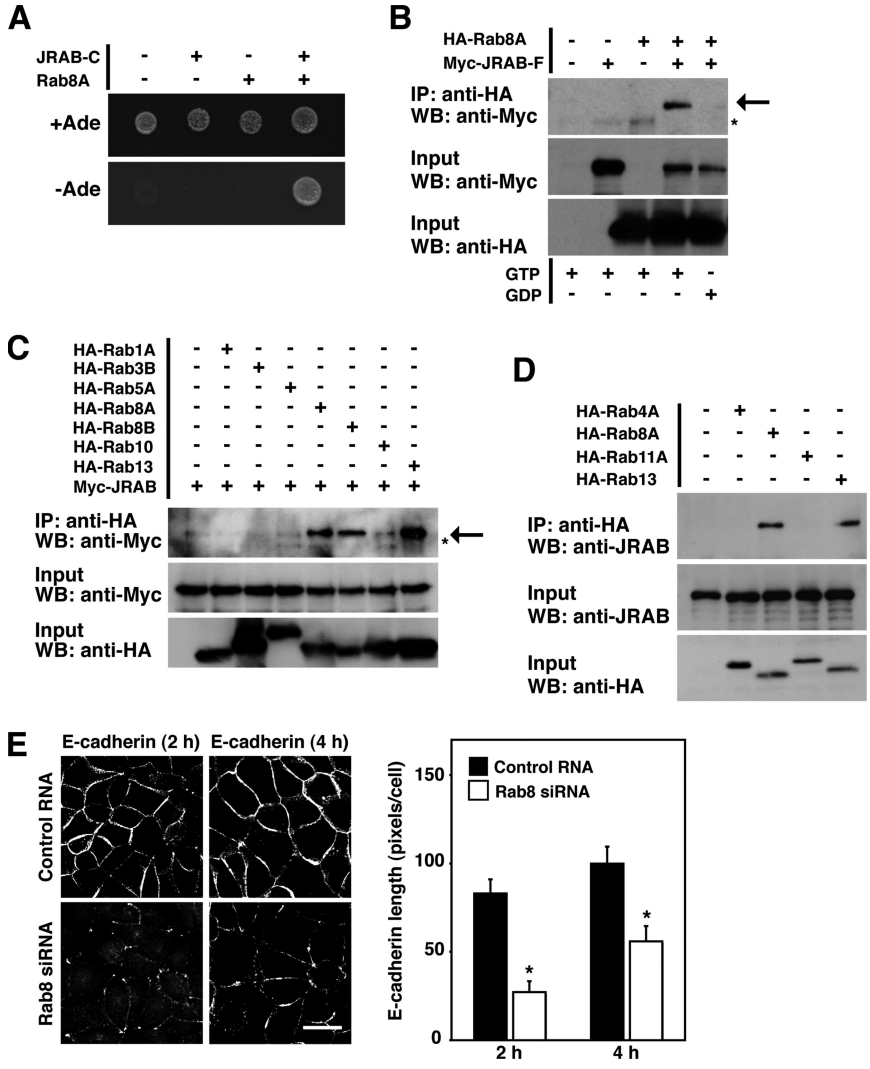

Figure 4. Rab8A is identified as another JRAB/MICAL-L2-binding protein that mediates the Rab13-independent transport of E-cadherin to the PM. (A) Yeast transformants carrying the bait vector (pGBDU or pGBDU-JRAB/MICAL-L2-C) and the prey vector (pACT2 or pACT2-Rab8A) were spotted on synthetic complete medium containing or lacking adenine to score for ADE2 reporter activity, and then they were incubated at 30°C for 3 d. (B) BHK cells expressing Myc-JRAB/MICAL-L2-F with HA-Rab8A were immunoprecipitated (IP) in the presence of either GTPγS (GTP) or GDP with an anti-HA antibody and subjected to Western blot (WB) analysis by using anti-Myc and anti-HA antibodies. The arrow indicates Myc-JRAB/MICAL-L2-F, and the asterisk indicates a nonspecific band. (C) BHK cells expressing Myc-JRAB/MICAL-L2 with HA-Rab1A, HA-Rab3B, HA-Rab5A, HA-Rab8A, HA-Rab8B, HA-Rab10, or HA-Rab13 were immunoprecipitated with an anti-HA antibody and subjected to Western blot analysis by using anti-Myc and anti-HA antibodies. The arrow indicates Myc-JRAB/MICAL-L2-F, and the asterisk indicates the nonspecific band. (D) MTD-1A cells expressing HA-Rab4A, HA-Rab8A, HA-Rab11A, or HA-Rab13 were immunoprecipitated with an anti-HA antibody and subjected to Western blot analysis by using anti-JRAB/MICAL-L2 and anti-HA antibodies. The results shown in A–D are representative of three independent experiments. (E) MDCK cells transfected with control RNA or Rab8A siRNA were subjected to a Ca^{2+}-switch assay, and then they were immunostained with an anti-E-cadherin antibody at the indicated time after Ca^{2+} restoration. Representative images of three independent experiments are shown. Bar, 20 μm. E-cadherin length is quantified and shown as the mean and SEM. The asterisks denote a significant difference between control RNA and Rab8A siRNA ($p < 0.05$).

value (>800 Ωcm²). However, these cells differed in the kinetics of TER development during a Ca^{2+}-switch assay. Consistent with our previous observations in MTD-1A cells (Terai *et al*., 2006), the development of TER after 6 and 12 h of Ca^{2+} restoration was impaired in JRAB/MICAL-L2–depleted MDCK I cells compared with control cells (Figure 5E). Although we cannot formally exclude the involvement of MICAL-1 and MICAL-L1 at present, these results suggest that JRAB/MICAL-L2 is a key MICAL family member in the assembly of functional TJs.

Rab8 Competes with Rab13 for the Binding of JRAB/MICAL-L2

If JRAB/MICAL-L2 physiologically interacted with both Rab8 and Rab13, it could make either a tripartite complex (Rab8-JRAB/MICAL-L2-Rab13) or two separate complexes (Rab8-JRAB/MICAL-L2 and Rab13-JRAB/MICAL-L2). To discriminate between these possibilities, we first tried to identify the Rab8A- and Rab13-binding domains within JRAB/MICAL-L2-C. For this purpose, we divided JRAB/MICAL-L2-C (amino acids 806-1009) into two parts: JRAB/MICAL-L2-CC, with the coiled-coil (CC) domain (amino acids 806–912), and JRAB/MICAL-L2-CT, without the CC domain (amino acids 913-1009) (Figure 6A). We then examined their binding to Rab8A and Rab13 by coimmunoprecipitation. Although Myc-JRAB/MICAL-L2-C efficiently interacted with Rab8A, neither Myc-JRAB/MICAL-L2-CC nor Myc-JRAB/MICAL-L2-CT bound Rab8A (Figure 6B). Similarly, Myc-JRAB/MICAL-L2-C, but not Myc-JRAB/MICAL-L2-CC and Myc-JRAB/MICAL-L2-CT, bound Rab13 (Figure 6B).

The inability to differentiate the Rab8-binding domain from the Rab13-binding domain prompted us to examine whether Rab8 competed with Rab13 for the binding of JRAB/MICAL-L2. To this end, we first attempted to produce Rab8 and Rab13 proteins in *E. coli*, but both proteins were only partially soluble, and the purified proteins did not function in our in vitro JRAB/MICAL-L2-binding assay. Therefore, we coexpressed a constant amount of HA-tagged JRAB/MICAL-L2 (HA-JRAB/MICAL-L2) and Myc-tagged Rab13 (Myc-Rab13) into BHK cells together with increased amounts of Myc-tagged Rab8A (Myc-Rab8A), and we assessed the interaction of JRAB/MICAL-L2 with Rab13 and Rab8A by coimmunoprecipitation. Without Rab8A expression, Rab13 was efficiently coimmunoprecipitated with JRAB/MICAL-L2. However, the coexpression of Rab8A inhibited the interaction of JRAB/MICAL-L2 with Rab13 in a dose-dependent manner (Figure 6C). Next, we performed the reverse coimmunoprecipitation

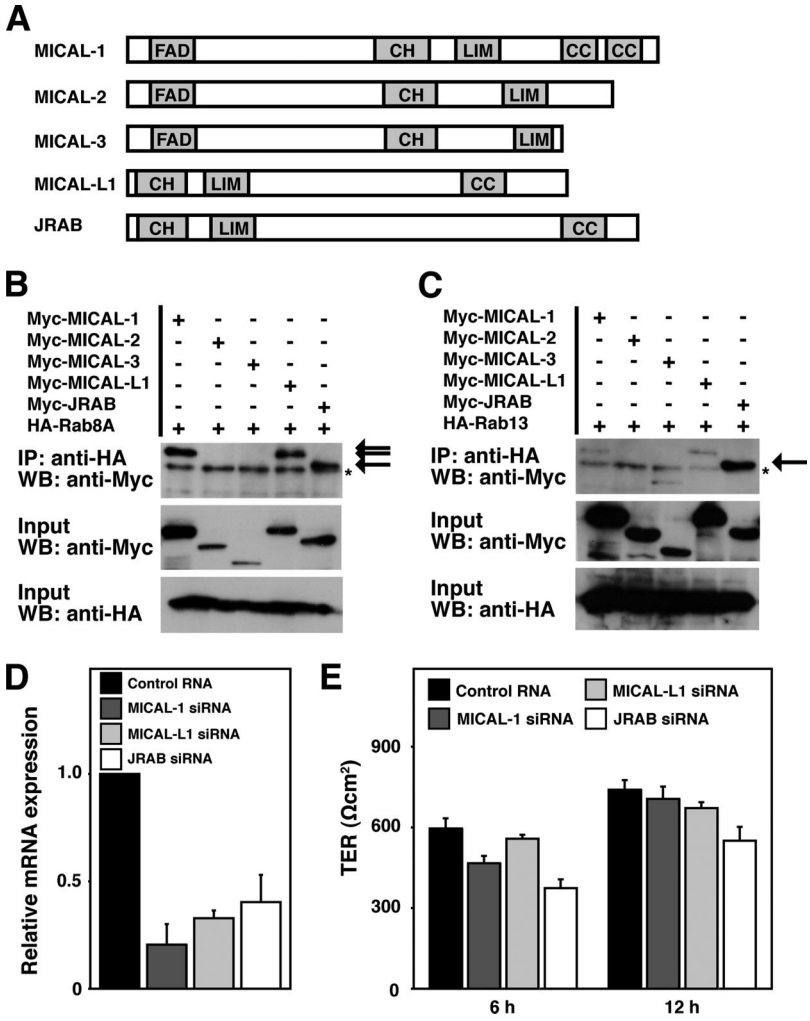

Figure 5. MICAL family proteins specifically interact with Rab family proteins. (A) Structures of MICAL family proteins. FAD, FAD-binding domain; CH, calponin homology domain; LIM, LIM domain; and CC, coiled-coil domain. (B and C) BHK cells expressing Myc-MICAL-1, Myc-MICAL-2, Myc-MICAL-3, Myc-MICAL-L1, or Myc-JRAB/MICAL-L2 with HA-Rab8A (B) or HA-Rab13 (C) were IP with an anti-HA antibody and subjected to WB analysis by using anti-Myc and anti-HA antibodies. The arrows indicate Myc-MICAL-1, Myc-MICAL-L1, and Myc-JRAB/MICAL-L2, and the asterisks indicate nonspecific bands. The results shown in B and C are representative of three independent experiments. (D) Total RNA was prepared from MDCK I cells transfected with control RNA, MICAL-1 siRNA, MICAL-L1 siRNA, or JRAB/MICAL-L2 siRNA, and the relative mRNA expression of MICAL-1, MICAL-L1, and JRAB/MICAL-L2 to GAPDH was determined by quantitative real-time PCR analysis. Data were shown as the mean and SEM for triplicate determinations. The mean expression of MICAL-1, MICAL-L1, and JRAB/MICAL-L2 mRNA in MDCK I cells transfected with control RNA was set to 1. (E) MDCK I cells transfected with control RNA, MICAL-1 siRNA, MICAL-L1 siRNA, and JRAB/MICAL-L2 siRNA were subjected to Ca^{2+}-switch assay. TER was measured at 6 and 12 h after Ca^{2+} restoration. The results shown are the mean and SEM of three independent experiments.

to examine whether Rab13 competed with Rab8 for the binding of JRAB/MICAL-L2. Like Rab8A, the increasing amount of Rab13 expression efficiently displaced the JRAB/MICAL-L2-bound Rab8A (Figure 6D). These results suggested that Rab8 competed with Rab13 for the binding to JRAB/MICAL-L2 and formed the distinct JRAB/MICAL-L2 complex from Rab13 within a single cell.

JRAB/MICAL-L2 Interacts with Rab8 and Rab13 at Specific Intracellular Sites

We then analyzed the intracellular localization of Rab8, Rab13, and JRAB/MICAL-L2 in MDCK cells. In agreement with previous reports (Huber *et al*., 1993b; Marzesco *et al*., 2002; Ang *et al*., 2004; Terai *et al*., 2006), Rab8A, Rab13, and JRAB/MICAL-L2 were all detected at perinuclear membrane structures, vesicular structures in the cytosol, and PM (Figure 7, A and B). To characterize the intracellular sites where JRAB/MICAL-L2 interacted with Rab8A and Rab13, FLAG-tagged Rab8A (FLAG-Rab8A) or FLAG-tagged Rab13 (FLAG-Rab13) was coexpressed with HA-JRAB/MICAL-L2 and colabeled with markers for the Golgi (Golgi 58K), the early endosome (EEA1), the late endosome (M6PR), the recycling endosome (Alexa-Tf), and the PM (ZO-1). Although FLAG-Rab8A colocalized with HA-JRAB/MICAL-L2 at the sites labeled with the internalized Alexa-Tf, Golgi 58K, and ZO-1, a closer spatial relationship between FLAG-Rab8A, HA-JRAB/MICAL-L2, and the internalized Alexa-Tf was observed (Figure 7A). Similarly, FLAG-Rab13, HA-JRAB/MICAL-L2, and ZO-1 showed a closer spatial relationship, albeit FLAG-Rab13 also associated with HA-JRAB/MICAL-L2 at the internalized Alexa-Tf and Golgi 58K-positive sites (Figure 7B). To further define the interaction sites of JRAB/MICAL-L2 with Rab8A and Rab13, HA-JRAB/MICAL-L2 was coexpressed with a GTP hydrolysis-defective mutant of FLAG-Rab8A (FLAG-Rab8A Q67L) or FLAG-Rab13 (FLAG-Rab13 Q67L) in MDCK cells. Although an intracellular distribution pattern of FLAG-Rab8A Q67L and FLAG-Rab13 Q67L was very similar to that of FLAG-Rab8A and FLAG-Rab13, the distinct localization of Rab8A-JRAB/MICAL-L2 and Rab13-JRAB/MICAL-L2 complexes was frequently emphasized in the presence of FLAG-Rab8A Q67L and FLAG-Rab13 Q67L (Figure 7, C and D).

Rab8-JRAB/MICAL-L2 and Rab13-JRAB/MICAL-L2 Complexes Are Involved in the Recycling of E-Cadherin and Occludin to the PM

The existence of distinct Rab8-JRAB/MICAL-L2 and Rab13-JRAB/MICAL-L2 complexes within a single cell prompted us to examine the molecular mechanism of how two JRAB/MICAL-L2 complexes control the transport of E-cadherin and occludin to the PM. To define the transport routes taken

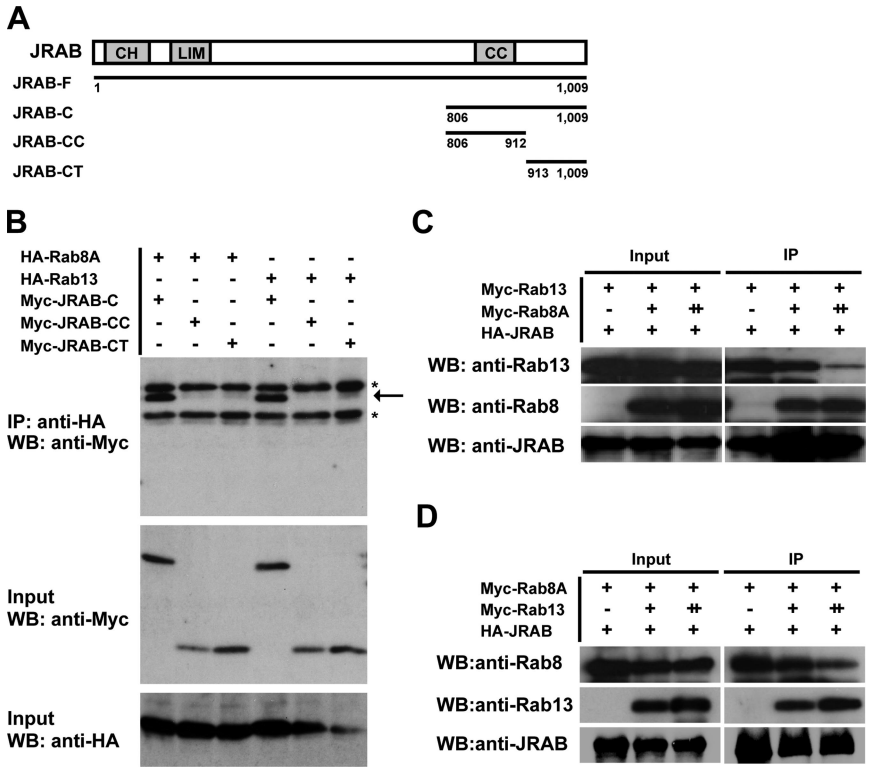

Figure 6. Rab8 competes with Rab13 for the binding to JRAB/MICAL-L2. (A) Structures of JRAB/MICAL-L2-C, JRAB/MICAL-L2-CC, and JRAB/MICAL-L2-CT proteins. CH, calponin homology domain; LIM, LIM domain; and CC, coiled-coil domain. (B) BHK cells expressing Myc-JRAB/MICAL-L2-C, Myc-JRAB/MICAL-L2-CC, or Myc-JRAB/MICAL-L2-CT with HA-Rab8A or HA-Rab13 were IP with an anti-HA antibody and subjected to WB analysis by using anti-Myc and anti-HA antibodies. The arrow indicates Myc-JRAB/MICAL-L2-C, and the asterisks indicate nonspecific bands. (C) BHK cells cotransfected with pCI-neo-HA-JRAB/MICAL-L2 (+, 2.0 μg) and pCI-neo-Myc-Rab13 (+, 1.0 μg) together with pCI-neo-Myc (−, 2.0 μg), pCI-neo-Myc + pCI-neo-Myc-Rab8A (+, 1.5 + 0.5 μg), or pCI-neo-Myc-Rab8A (++, 2.0 μg) were IP with an anti-HA antibody and subjected to WB analysis by using anti-Rab13, anti-Rab8, and anti-JRAB/MICAL-L2 antibodies. (D) BHK cells cotransfected with pCI-neo-HA-JRAB/MICAL-L2 (+, 2.0 μg) and pCI-neo-Myc-Rab8A (+, 1.0 μg) together with pCI-neo-Myc (−, 2.0 μg), pCI-neo-Myc + pCI-neo-Myc-Rab13 (+, 1.5 + 0.5 μg), or pCI-neo-Myc-Rab13 (++, 2.0 μg) were IP and subjected to WB analysis as described in C. The results shown in B–D are representative of three independent experiments.

by E-cadherin and occludin, we first performed a Ca^{2+}-switch assay in the presence of cycloheximide to stop de novo protein synthesis and expose the role of the PNC. When MDCK cells were subjected to a Ca^{2+}-switch assay in the presence of cycloheximide, E-cadherin and occludin were internalized from the PM and accumulated in the PNC, where the internalized Alexa-Tf was also detected, after Ca^{2+} removal (Figure 8A). Then, they were gradually transported from the PNC to the PM during 3 h of Ca^{2+} restoration and detected both in the PNC and PM at 1 and 1.5 h after Ca^{2+} restoration (Figure 8A). We next examined the colocalization of Rab8-JRAB/MICAL-L2 and Rab13-JRAB/MICAL-L2 complexes with E-cadherin and occludin at 1 h after Ca^{2+} restoration. When MDCK cells coexpressing Myc-JRAB/MICAL-L2 with FLAG-Rab8A or FLAG-Rab13 were examined at 1 h after Ca^{2+} restoration, the FLAG-Rab8A-Myc-JRAB/MICAL-L2 complex was colocalized with E-cadherin both at the PNC and PM, whereas the cytosolic vesicular structures containing all of FLAG-Rab8A, Myc-JRAB/MICAL-L2, and E-cadherin were barely evident (Figure 8B). Similarly, the colocalization of FLAG-Rab13-Myc-JRAB/MICAL-L2 complex with occludin was also detected both at the PNC and PM, but hardly in the cytosolic vesicular structures, at 1 h after Ca^{2+} restoration (Figure 8B).

To define the role of Rab8-JRAB/MICAL-L2 and Rab13-JRAB/MICAL-L2 complexes in the recycling of E-cadherin and occludin from the PNC to the PM, we depleted JRAB/MICAL-L2, Rab8A, and Rab13 in MDCK cells, and we performed a Ca^{2+}-switch assay in the presence of cycloheximide. Compared with control MDCK cells, the recycling of both E-cadherin and occludin was inhibited in JRAB/MICAL-L2-depleted cells at 1 h after Ca^{2+} restoration (Figure 8C). Knockdown of Rab8A and Rab13 suppressed the recycling of E-cadherin and occludin at 1 h after Ca^{2+} restoration, respectively (Figure 8, D and E). To get an insight into the functional sites for the Rab8A-JRAB/MICAL-L2 and Rab13-JRAB/MICAL-L2 complexes, we next measured the JRAB/MICAL-L2-E-cadherin and JRAB/MICAL-L2-occludin colocalized area at the PNC and PM in control, Rab8A-depleted, and Rab13-depleted cells at 1 h after Ca^{2+} restoration. Consistent with the decrease in the mean E-cadherin and occludin length (Figure 8, D and E), the JRAB/MICAL-L2-E-cadherin and JRAB/MICAL-L2-occludin colocalized area at the PM was also decreased in Rab8A-depleted and Rab13-depleted cells, respectively. However, the ratio of the JRAB/MICAL-L2-E-cadherin colocalized area at the PNC to that at the PM was slightly decreased in Rab8A-depleted cells (0.58 ± 0.39) compared with control cells (0.61 ± 0.16) (Figure 8D), whereas that of JRAB/MICAL-L2-occludin was increased in Rab13-depleted cells (0.69 ± 0.35) compared with control cells (0.21 ± 0.12) (Figure 8E). These opposite changes in the ratio of colocalized area suggest the distinct roles of Rab8A-JRAB/MICAL-L2 and Rab13-JRAB/MICAL-L2 complexes at the PNC and PM.

DISCUSSION

The formation and destruction of TJs and AJs are essential for the physiological development of multicellular organisms. Failure in their regulation is manifested in a variety of diseases, such as tissue fibrosis and tumor invasion/metastasis. To gain insight into the molecular mechanisms of TJ and AJ assembly, we previously showed that Rab13 and JRAB/MICAL-L2 mediated the endocytic recycling of occludin and regulated the assembly of functional TJs (Morimoto *et al.*, 2005; Terai *et al.*, 2006). Our present study revealed five key findings. First, JRAB/MICAL-L2 regulated the transport of both TJ and AJ proteins to the PM, whereas Rab13 specifically mediated that of TJ but not AJ proteins. Second, JRAB/MICAL-L2 also interacted with Rab8, which mediated the Rab13-independent transport of AJ protein to the

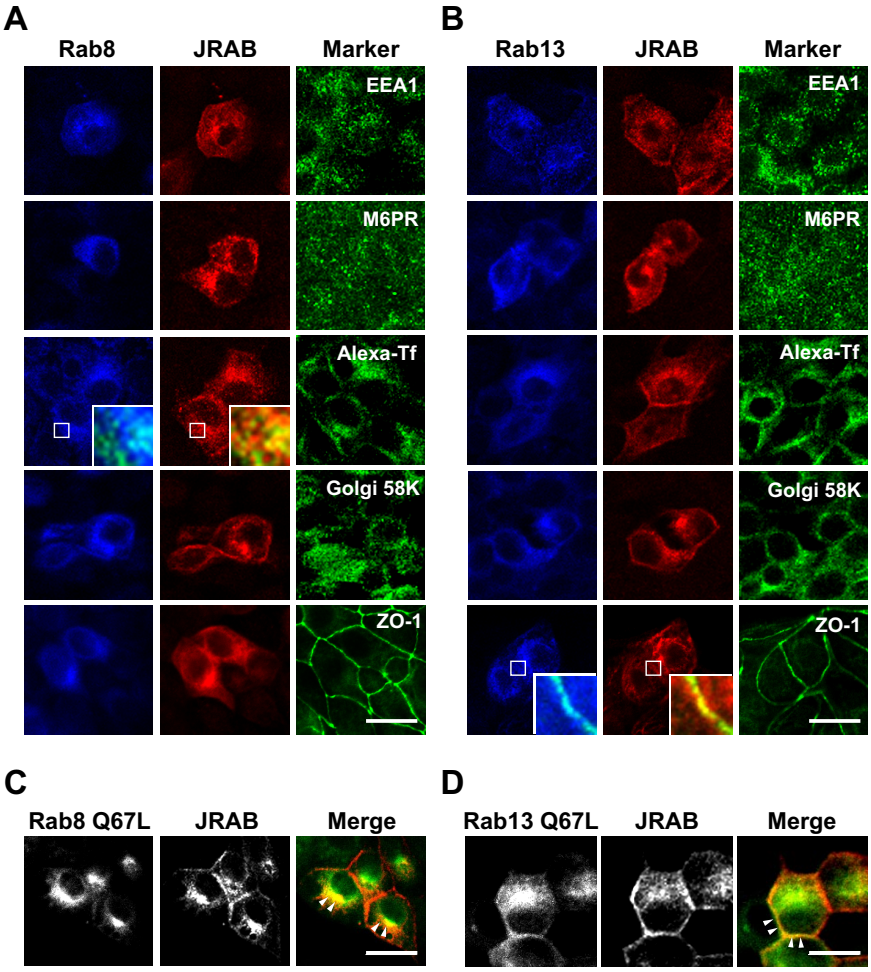

Figure 7. JRAB/MICAL-L2 interacts with Rab8 and Rab13 at specific intracellular sites. (A and B) MDCK cells coexpressing HA-JRAB/MICAL-L2 with FLAG-Rab8A (A) or FLAG-Rab13 (B) were triple labeled with anti-FLAG antibody, anti-HA antibody, and organella markers (anti-EEA1 antibody, anti-M6PR antibody, Alexa-Tf, anti-Golgi 58K antibody, and anti-ZO-1 antibody). Magnified images in inserts show the notable colocalization with organella markers. Bars, 20 μm. (C and D) MDCK cells coexpressing HA-JRAB/MICAL-L2 with FLAG-Rab8A Q67L (C) or FLAG-Rab13 Q67L (D) were double labeled with anti-FLAG and anti-HA antibodies. In the merged images, Rab8A Q67L/Rab13 Q67L was green and JRAB was red. The arrowheads indicate the sites of prominent colocalization. Bars, 20 μm. The results shown in A–D are representative of three independent experiments.

PM. Third, Rab8 and Rab13 competed with each other to bind JRAB/MICAL-L2. Fourth, JRAB/MICAL-L2 mainly associated with Rab8 and Rab13 at the PNC and PM, respectively. Fifth, depletion of Rab8 and Rab13 impaired the colocalization of JRAB/MICAL-L2 with AJ protein at the PNC and TJ protein at the PM, respectively. Collectively, these results suggest that JRAB/MICAL-L2 coordinates the assembly of AJ and TJ by forming the distinct Rab8-JRAB/MICAL-L2 and Rab13-JRAB/MICAL-L2 complexes (Figure 9).

A key finding in the present study is the identification of JRAB/MICAL-L2 as a shared Rab effector protein that forms mutually distinct complexes with Rab8 and Rab13. To ensure the proper transport and maintain the identity of intracellular membrane compartments, the action of each Rab protein needs to be coordinated with other Rab proteins (Markgraf *et al*., 2007). The Rab coupling is potentially mediated by Rab-binding proteins that can interact with multiple Rab proteins. Currently, two types of these Rab-binding proteins are identified. One type comprises Rab-binding proteins that function as an effector protein for one Rab protein and as a GTP exchange factor (GEF) for another Rab protein. The identification of this type of Rab-binding proteins that include Sec2 and the class C-VPS/HOPS complex leads to the concept of a Rab cascade (Ortiz *et al*., 2002; Rink *et al*., 2005). Another type is a divalent Rab effector protein that binds simultaneously to two Rab proteins associated with compartments in dynamic continuity. Rabaptin5, Rabenosyn5, and Rabip4′ are able to interact simultaneously with Rab4 and Rab5, and they are likely involved in the coordination of the endocytic recycling pathway and the organization of Rab4 and Rab5 domains on endosomal membranes (Vitale *et al*., 1998; de Renzis *et al*., 2002; Fouraux *et al*., 2004). Although an increasing number of Rab effector proteins are reported to interact with closely related multiple Rab proteins (Fukuda, 2003), their functional significance still remains to be determined. To our knowledge, JRAB/MICAL-L2 is a novel type of Rab effector protein that associate with closely related Rab proteins forming mutually exclusive complexes.

In the present study, we found that JRAB/MICAL-L2 controlled the transport of claudins, occludin, and E-cadherin to the PM, and Rab8 regulated the Rab13-independent transport of E-cadherin to the PM. Although knockdown of Rab8 also impaired the transport of claudins and occludin (Supplemental Figure S4, D and E), this could be caused by the inhibition of E-cadherin transport as TJ protein transport was depend on AJ protein transport in a Ca^{2+}-switch model (Yap *et al*., 1997; Takai and Nakanishi, 2003). The present study adds JRAB/MICAL-L2 and Rab8 to a growing list of regulatory molecules for E-cadherin trafficking (Bryant and Stow, 2004; D'Souza-Schorey, 2005; Ivanov *et al*., 2005). Although Rab8 is functionally linked to epithelial specific clathrin adaptor complexes AP-1B and E-cadherin is initially recognized as an AP-1B-independent basolateral cargo (Miranda *et al*., 2001; Ang *et al*., 2003; Fölsch, 2005), a recent observation that phosphatidylinositol-4-phosphate 5-kinase

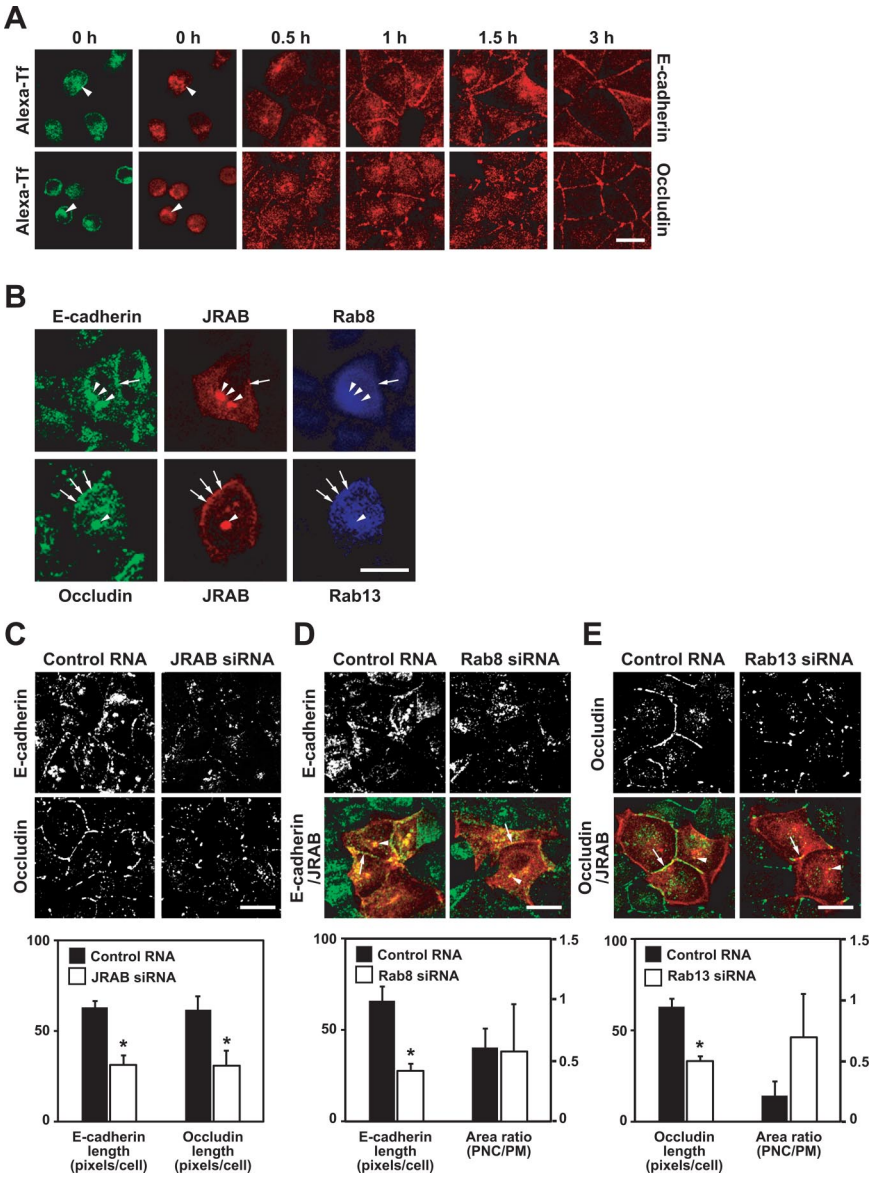

Figure 8. Rab8-JRAB/MICAL-L2 and Rab13-JRAB/MICAL-L2 complexes are involved in the recycling of E-cadherin and occludin to the PM. (A) MDCK cells labeled with Alexa-Tf were subjected to a Ca^{2+}-switch assay in the presence of cycloheximide and then immunostained with anti-E-cadherin or anti-occludin antibody at the indicated time after Ca^{2+} restoration. The arrowheads indicate the overlap. Bar, 20 μm. (B) MDCK cells coexpressing HA-JRAB/MICAL-L2 with FLAG-Rab8A or FLAG-Rab13 were subjected to a Ca^{2+}-switch assay in the presence of cycloheximide, and then they were triple labeled with anti-HA, anti-FLAG, and anti-E-cadherin or anti-occludin antibodies at 1 h after Ca^{2+} restoration. The arrows and arrowheads indicate the colocalization at the PM and PNC, respectively. Bar, 20 μm. (C–E) MDCK cells transfected with control RNA or JRAB/MICAL-L2 siRNA (C), pCI-neo-HA-JRAB/MICAL-L2 with control RNA or Rab8A siRNA (D), or pCI-neo-HA-JRAB/MICAL-L2 with control RNA or Rab13 siRNA (E) were subjected to a Ca^{2+}-switch assay in the presence of cycloheximide and then immunostained with anti-E-cadherin, anti-occludin, and anti-HA antibodies at 1 h after Ca^{2+} restoration. E-cadherin or occludin length was quantified and shown as the mean and SEM. The asterisks denote a significant difference ($p < 0.05$). The ratio of JRAB/MICAL-L2-E-cadherin or JRAB/MICAL-L2-occludin colocalized area at the PNC to that at the PM was quantified and shown as the mean and SEM. The arrows and arrowheads indicate the colocalization at the PM and PNC, respectively. Bars, 20 μm. The images shown in A–E are representative of three independent experiments.

γ modulates the basolateral transport of E-cadherin and directly binds both E-cadherin and AP-1B supports our results (Ling *et al*., 2007). Furthermore, Rab8 is recently shown to colocalize with Rab11 and ARF6, both of which are implicated in the transport of E-cadherin, and it is functionally linked to ARF6 (Palacios *et al*., 2001; Lock and Stow, 2005; Hattula *et al*., 2006). Collectively, Rab8, Rab11, and ARF6 seem to coordinate the transport of E-cadherin to the PM. Although the exact nature of this coordination remains elusive, one possible explanation would be that Rab8, Rab11, and ARF6 sequentially act through the same transport pathway of E-cadherin. In this scenario, a cascade of Rab8, Rab11, and ARF6 would be expected. Alternatively, Rab8, Rab11, and ARF6 could simultaneously work on the distinct transport pathways of E-cadherin. This case would predict the existence of different populations of transport carriers containing E-cadherin.

Then, the question of how JRAB/MICAL-L2 works as a shared Rab8 and Rab13 effector protein on the transport of E-cadherin and occludin to the PM has naturally arisen. As JRAB/MICAL-L2 is directly or indirectly associated with actin cytoskeletons (Terai *et al*., 2006), we speculate the involvement of JRAB/MICAL-L2 in the membrane-actin cytoskeleton interactions, and we can formulate several models to explain the present results. Considering a widespread concept that Rab and its effector proteins can recruit myosin motors onto the transport carrier membranes (Seabra and Coudrier, 2004), Rab8-JRAB/MICAL-L2 and Rab13-JRAB/MICAL-L2 complexes could recruit myosin motors onto the transport carrier membranes containing E-cadherin and occludin, respectively. Although we did not detect the colocalization of Rab8-JRAB/MICAL-L2 and Rab13-JRAB/MICAL-L2 on the transport carriers, we cannot formally exclude this model at the moment. Alternatively, Rab8-JRAB/MICAL-L2 and Rab13-JRAB/MICAL-L2 complexes could mediate the membrane-actin cytoskeleton interactions at the PNC and PM, respectively. According to this model, Rab8-JRAB/MICAL-L2 complex would sort E-cadherin within the PNC membranes or generate E-cadherin transport carrier from the PNC, whereas Rab13-JRAB/MICAL-L2 complex would tether/dock/fuse occludin transport carrier with

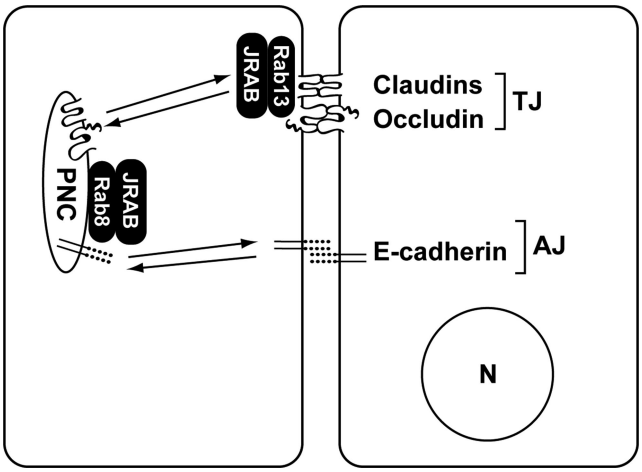

Figure 9. Schematic model for the action of Rab8-JRAB/MICAL-L2 and Rab13-JRAB/MICAL-L2 complexes in the assembly of AJs and TJs. Whereas the Rab8-JRAB/MICAL-L2 complex resided at the PNC mediates the recycling of E-cadherin to the PM and the assembly of AJs, the Rab13-JRAB/MICAL-L2 complex resided at the PM regulates the recycling of claudins and occludin to the PM and the formation of TJs. N, nucleus.

the PM. JRAB/MICAL-L2 would directly mediate these processes or scaffold the executing molecule(s) as it contains multiple protein–protein interaction domains. The further determination of the JRAB/MICAL-L2-interacting molecules would be essential for this model.

Another important question is how JRAB/MICAL-L2 controls its interaction with Rab8 and Rab13. Although the intracellular distribution of Rab8, Rab13, and JRAB/MICAL-L2 were overlapped at the PNC and PM, the Rab8-JRAB/MICAL-L2 and Rab13-JRAB/MICAL-L2 interactions were preferentially detected at the PNC and PM, respectively. Because Rab8 and Rab13 compete with each other for the interaction with JRAB/MICAL-L2 (Figure 6, C and D), there must exist the additional mechanism(s) to activate/stabilize the Rab8-JRAB/MICAL-L2 and Rab13-JRAB/MICAL-L2 interactions at the PNC and PM, respectively. Alternatively, the Rab8-JRAB/MICAL-L2 and Rab13-JRAB/MICAL-L2 interactions might be inactivated/prevented at the PM and PNC, respectively. In support of stabilizing mechanism for the Rab13-JRAB/MICAL-L2 interaction at the PM, JRAB/MICAL-L2 also interacted with actinin-4 and made the Rab13-JRAB/MICAL-L2-actinin-4 complex at TJs (our unpublished observations). Other potential stabilizing and/or preventing mechanisms for the Rab8-JRAB/MICAL-L2 and Rab13-JRAB/MICAL-L2 interactions are currently under investigation.

In accordance with the involvement of JRAB/MICAL-L2 in TJ and AJ assembly, a series of recent studies begin to reveal the potential role of MICAL family proteins in the regulation of invasive growth (Comoglio and Trusolino, 2002). MICAL-1, MICAL-2, and MICAL-3 are shown to function downstream of the Semaphorin 3 receptor Plexin A during axon guidance (Terman *et al*., 2002). The MICAL-2 isoforms (MICAL-2 PVa and PVb) are implicated in the progression of prostate cancer (Ashida *et al*., 2006). Consistent with the obligatory demand for extensive membrane trafficking and cytoskeletal rearrangement during invasive growth, the interactions of MICAL family proteins with Rab1, vimentin, and microtubules are also detected (Suzuki *et al*., 2002; Weide *et al*., 2003; Fischer *et al*., 2005).

In summary, our results suggest that JRAB/MICAL-L2 represents a novel type of a shared Rab effector protein that forms mutually distinct complexes with closely related Rab8 and Rab13. JRAB/MICAL-L2 interacts with the GTP-bound forms of Rab8 and Rab13 at the PNC and PM, respectively, and the Rab8-JRAB/MICAL-L2 and Rab13-JRAB/MICAL-L2 complexes coordinate the assembly of AJs and TJs through the regulation of Rab8-dependent E-cadherin transport and Rab13-dependent claudins/occludin transport.

ACKNOWLEDGMENTS

We thank Dr. W. Birchmeier for the MDCK cells, Dr. T. Tsukamoto for the MDCK I cells, and Dr. S. Tsukita for the MTD-1A cells and the anti-occludin (MOC37) antibody. This study was supported by Grants-in-Aid for Scientific Research (18590271 to N.N. and 15079207, 18390089 to T.S.) from the Ministry of Education, Culture, Sports, Science and Technology of Japan.

REFERENCES

Ang, A., Fölsch, H., Koivisto, U., Pypaert, M., and Mellman, I. (2003). The Rab8 GTPase selectively regulates AP-1B-dependent basolateral transport in polarized Madin-Darby canine kidney cells. J. Cell Biol. *163*, 339–350.

Ang, A., Taguchi, T., Francis, S., Fölsch, H., Murrells, L., Pypaert, M., Warren, G., and Mellman, I. (2004). Recycling endosomes can serve as intermediates during transport from the Golgi to the plasma membrane of MDCK cells. J. Cell Biol. *167*, 531–543.

Ashida, S. *et al*. (2006). Expression of novel molecules, MICAL2-PV (MICAL2 prostate cancer variants), increases with high Gleason score and prostate cancer progression. Clin. Cancer Res. *12*, 2767–2773.

Balzac, F., Avolio, M., Degani, S., Kaverina, I., Torti, M., Silengo, L., Small, J., and Retta, S. (2005). E-cadherin endocytosis regulates the activity of Rap *1*, a traffic light GTPase at the crossroads between cadherin and integrin function. J. Cell Sci. *118*, 4765–4783.

Bruewer, M., Utech, M., Ivanov, A., Hopkins, A., Parkos, C., and Nusrat, A. (2005). Interferon-γ induces internalization of epithelial tight junction proteins via a macropinocytosis-like process. FASEB J. *19*, 923–933.

Bryant, D., and Stow, J. (2004). The ins and outs of E-cadherin trafficking. Trends Cell Biol. *14*, 427–434.

Chabrillat, M., Wilhelm, C., Wasmeier, C., Sviderskaya, E., Louvard, D., and Coudrier, E. (2005). Rab8 regulates the actin-based movement of melanosomes. Mol. Biol. Cell *16*, 1640–1650.

Comoglio, P., and Trusolino, L. (2002). Invasive growth: from development to metastasis. J. Clin. Invest. *109*, 857–862.

D'Souza-Schorey, C. (2005). Disassembling adherens junctions: breaking up is hard to do. Trends Cell Biol. *15*, 19–26.

de Renzis, S., Sönnichsen, B., and Zerial, M. (2002). Divalent Rab effectors regulate the sub-compartmental organization and sorting of early endosomes. Nat. Cell Biol. *4*, 124–133.

Di Giovanni, S., De Biase, A., Yakovlev, A., Finn, T., Beers, J., Hoffman, E., and Faden, A. (2005). In vivo and in vitro characterization of novel neuronal plasticity factors identified following spinal cord injury. J. Biol. Chem. *280*, 2084–2091.

Ebnet, K., Suzuki, A., Ohno, S., and Vestweber, D. (2004). Junctional adhesion molecules (JAMs): more molecules with dual functions? J. Cell Sci. *117*, 19–29.

Fischer, J., Weide, T., and Barnekow, A. (2005). The MICAL proteins and rab 1, a possible link to the cytoskeleton? Biochem. Biophys. Res. Commun. *328*, 415–423.

Fölsch, H. (2005). The building blocks for basolateral vesicles in polarized epithelial cells. Trends Cell Biol. *15*, 222–228.

Fouraux, M., Deneka, M., Ivan, V., van der Heijden, A., Raymackers, J., van Suylekom, D., van Venrooij, W., van der Sluijs, P., and Pruijn, G. (2004). Rabip4′ is an effector of rab5 and rab4 and regulates transport through early endosomes. Mol. Biol. Cell *15*, 611–624.

Fukuda, M. (2003). Distinct Rab binding specificity of Rim1, Rim2, rabphilin, and Noc2. Identification of a critical determinant of Rab3A/Rab27A recognition by Rim2. J. Biol. Chem. *278*, 15373–15380.

Gonzalez-Mariscal, L., Betanzos, A., Nava, P., and Jaramillo, B. (2003). Tight junction proteins. Prog. Biophys. Mol. Biol. *81*, 1–44.

Harhaj, N., Barber, A., and Antonetti, D. (2002). Platelet-derived growth factor mediates tight junction redistribution and increases permeability in MDCK cells. J. Cell. Physiol. *193*, 349–364.

Hattula, K., and Peränen, J. (2000). FIP-2, a coiled-coil protein, links Huntingtin to Rab8 and modulates cellular morphogenesis. Curr. Biol. *10*, 1603–1606.

Hattula, K., Furuhjelm, J., Tikkanen, J., Tanhuanpaa, K., Laakkonen, P., and Peranen, J. (2006). Characterization of the Rab8-specific membrane traffic route linked to protrusion formation. J. Cell Sci. *119*, 4866–4877.

Hopkins, A., Walsh, S., Verkade, P., Boquet, P., and Nusrat, A. (2003). Constitutive activation of Rho proteins by CNF-1 influences tight junction structure and epithelial barrier function. J. Cell Sci. *116*, 725–742.

Huber, L., de Hoop, M., Dupree, P., Zerial, M., Simons, K., and Dotti, C. (1993a). Protein transport to the dendritic plasma membrane of cultured neurons is regulated by rab8p. J. Cell Biol. *123*, 47–55.

Huber, L., Pimplikar, S., Parton, R., Virta, H., Zerial, M., and Simons, K. (1993b). Rab8, a small GTPase involved in vesicular traffic between the TGN and the basolateral plasma membrane. J. Cell Biol. *123*, 35–45.

Ivanov, A., Nusrat, A., and Parkos, C. (2004). Endocytosis of epithelial apical junctional proteins by a clathrin-mediated pathway into a unique storage compartment. Mol. Biol. Cell *15*, 176–188.

Ivanov, A., Nusrat, A., and Parkos, C. (2005). Endocytosis of the apical junctional complex: mechanisms and possible roles in regulation of epithelial barriers. Bioessays *27*, 356–365.

James, P., Halladay, J., and Craig, E. (1996). Genomic libraries and a host strain designed for highly efficient two-hybrid selection in yeast. Genetics *144*, 1425–1436.

Kartenbeck, J., Schmelz, M., Franke, W., and Geiger, B. (1991). Endocytosis of junctional cadherins in bovine kidney epithelial (MDBK) cells cultured in low Ca^{2+} ion medium. J. Cell Biol. *113*, 881–892.

Köhler, K., Louvard, D., and Zahraoui, A. (2004). Rab13 regulates PKA signaling during tight junction assembly. J. Cell Biol. *165*, 175–180.

Lau, A., and Mruk, D. (2003). Rab8B GTPase and junction dynamics in the testis. Endocrinology *144*, 1549–1563.

Le, T., Yap, A., and Stow, J. (1999). Recycling of E-cadherin: a potential mechanism for regulating cadherin dynamics. J. Cell Biol. *146*, 219–232.

Ling, K., Bairstow, S., Carbonara, C., Turbin, D., Huntsman, D., and Anderson, R. (2007). Type Iγ phosphatidylinositol phosphate kinase modulates adherens junction and E-cadherin trafficking via a direct interaction with μ1B adaptin. J. Cell Biol. *176*, 343–353.

Lock, J., and Stow, J. (2005). Rab11 in recycling endosomes regulates the sorting and basolateral transport of E-cadherin. Mol. Biol. Cell *16*, 1744–1755.

Markgraf, D., Peplowska, K., and Ungermann, C. (2007). Rab cascades and tethering factors in the endomembrane system. FEBS Lett. *581*, 2125–2130.

Marzesco, A., Dunia, I., Pandjaitan, R., Recouvreur, M., Dauzonne, D., Benedetti, E., Louvard, D., and Zahraoui, A. (2002). The small GTPase Rab13 regulates assembly of functional tight junctions in epithelial cells. Mol. Biol. Cell *13*, 1819–1831.

Matsuda, M., Kubo, A., Furuse, M., and Tsukita, S. (2004). A peculiar internalization of claudins, tight junction-specific adhesion molecules, during the intercellular movement of epithelial cells. J. Cell Sci. *117*, 1247–1257.

Miranda, K., Khromykh, T., Christy, P., Le, T., Gottardi, C., Yap, A., Stow, J., and Teasdale, R. (2001). A dileucine motif targets E-cadherin to the basolateral cell surface in Madin-Darby canine kidney and LLC-PK1 epithelial cells. J. Biol. Chem. *276*, 22565–22572.

Morimoto, S., Nishimura, N., Terai, T., Manabe, S., Yamamoto, Y., Shinahara, W., Miyake, H., Tashiro, S., Shimada, M., and Sasaki, T. (2005). Rab13 mediates the continuous endocytic recycling of occludin to the cell surface. J. Biol. Chem. *280*, 2220–2228.

Nelson, W. (2003). Adaptation of core mechanisms to generate cell polarity. Nature *422*, 766–774.

Ortiz, D., Medkova, M., Walch-Solimena, C., and Novick, P. (2002). Ypt32 recruits the Sec4p guanine nucleotide exchange factor, Sec2p, to secretory vesicles; evidence for a Rab cascade in yeast. J. Cell Biol. *157*, 1005–1015.

Palacios, F., Price, L., Schweitzer, J., Collard, J., and D'Souza-Schorey, C. (2001). An essential role for ARF6-regulated membrane traffic in adherens junction turnover and epithelial cell migration. EMBO J. *20*, 4973–4986.

Pfeffer, S., and Aivazian, D. (2004). Targeting Rab GTPases to distinct membrane compartments. Nat. Rev. Mol. Cell Biol. *5*, 886–896.

Powell, R., and Temesvari, L. (2004). Involvement of a Rab8-like protein of *Dictyostelium discoideum*, Sas1, in the formation of membrane extensions, secretion and adhesion during development. Microbiology *150*, 2513–2525.

Ren, M., Zeng, J., De Lemos-Chiarandini, C., Rosenfeld, M., Adesnik, M., and Sabatini, D. (1996). In its active form, the GTP-binding protein rab8 interacts with a stress-activated protein kinase. Proc. Natl. Acad. Sci. USA *93*, 5151–5155.

Rink, J., Ghigo, E., Kalaidzidis, Y., and Zerial, M. (2005). Rab conversion as a mechanism of progression from early to late endosomes. Cell *122*, 735–749.

Seabra, M., and Coudrier, E. (2004). Rab GTPases and myosin motors in organelle motility. Traffic *5*, 393–399.

Suzuki, T., Nakamoto, T., Ogawa, S., Seo, S., Matsumura, T., Tachibana, K., Morimoto, C., and Hirai, H. (2002). MICAL, a novel CasL interacting molecule, associates with vimentin. J. Biol. Chem. *277*, 14933–14941.

Takai, Y., Sasaki, T., and Matozaki, T. (2001). Small GTP-binding proteins. Physiol. Rev. *81*, 153–208.

Takai, Y., and Nakanishi, H. (2003). Nectin and afadin: novel organizers of intercellular junctions. J. Cell Sci. *116*, 17–27.

Takeichi, M. (1995). Morphogenetic roles of classic cadherins. Curr. Opin. Cell Biol. *7*, 619–627.

Terai, T., Nishimura, N., Kanda, I., Yasui, N., and Sasaki, T. (2006). JRAB/MICAL-L2 is a junctional Rab13-binding protein mediating the endocytic recycling of occludin. Mol. Biol. Cell *17*, 2465–2475.

Terman, J., Mao, T., Pasterkamp, R., Yu, H., and Kolodkin, A. (2002). MICALs, a family of conserved flavoprotein oxidoreductases, function in plexin-mediated axonal repulsion. Cell *109*, 887–900.

Tsukita, S., Furuse, M., and Itoh, M. (2001). Multifunctional strands in tight junctions. Nat. Rev. Mol. Cell Biol. *2*, 285–293.

Utech, M., Ivanov, A., Samarin, S., Bruewer, M., Turner, J., Mrsny, R., Parkos, C., and Nusrat, A. (2005). Mechanism of IFN-γ-induced endocytosis of tight junction proteins: myosin II-dependent vacuolarization of the apical plasma membrane. Mol. Biol. Cell *16*, 5040–5052.

Vasioukhin, V., Bauer, C., Yin, M., and Fuchs, E. (2000). Directed actin polymerization is the driving force for epithelial cell-cell adhesion. Cell *100*, 209–219.

Vitale, G., Rybin, V., Christoforidis, S., Thornqvist, P., McCaffrey, M., Stenmark, H., and Zerial, M. (1998). Distinct Rab-binding domains mediate the interaction of Rabaptin-5 with GTP-bound Rab4 and Rab5. EMBO J. *17*, 1941–1951.

Weide, T., Teuber, J., Bayer, M., and Barnekow, A. (2003). MICAL-1 isoforms, novel rab1 interacting proteins. Biochem. Biophys. Res. Commun. *306*, 79–86.

Yamamoto, Y., Nishimura, N., Morimoto, S., Kitamura, H., Manabe, S., Kanayama, H., Kagawa, S., and Sasaki, T. (2003). Distinct roles of Rab3B and Rab13 in the polarized transport of apical, basolateral, and tight junctional membrane proteins to the plasma membrane. Biochem. Biophys. Res. Commun. *308*, 270–275.

Yap, A., Brieher, W., and Gumbiner, B. (1997). Molecular and functional analysis of cadherin-based adherens junctions. Annu. Rev. Cell Dev. Biol. *13*, 119–146.

Zahraoui, A., Joberty, G., Arpin, M., Fontaine, J., Hellio, R., Tavitian, A., and Louvard, D. (1994). A small rab GTPase is distributed in cytoplasmic vesicles in non polarized cells but colocalizes with the tight junction marker ZO-1 in polarized epithelial cells. J. Cell Biol. *124*, 101–115.

Zerial, M., and McBride, H. (2001). Rab proteins as membrane organizers. Nat. Rev. Mol. Cell Biol. *2*, 107–117.